The elastohydrodynamics of a simplified model of human birth

Roseanna Gossmann

Department of Mathematics
Tulane University
New Orleans, LA

April 10, 2018

Collaborators

Megan C. Leftwich, The George Washington University
Alexa Baumer, The George Washington University
Lisa Fauci, Tulane University

Motivation

A better understanding of the mechanics of human birth may decrease the incidence of unnecessary surgical delivery.

Considering Fluid Dynamics Is Essential

Amniotic fluid is highly variable

- in volume [1]
- in rheological properties [2]

It is unknown how these fluid properties affect the transfer of force from the uterus onto the baby during delivery.

Fluid dynamics were shown to significantly affect the force necessary for delivery in a model vacuum-assisted delivery. [3]

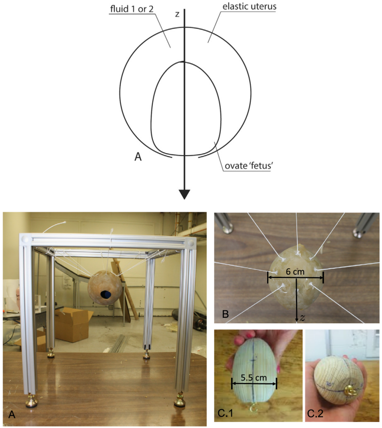

Experimental set-up at Leftwich laboratory for model vacuum-assisted delivery. [3]

[1] Brace, Wolf, *American J. of Obstetrics and Gynecology*, 1989
[2] Uyeno, *J. of Biological Chemistry*, 1919
[3] Lehn, Baumer, Leftwich, *J. of Biomechanics*, 2016

A Simplified Physical Experiment

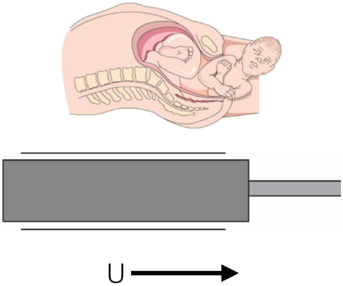

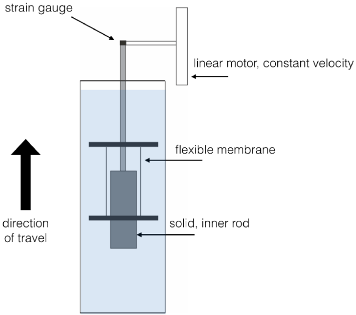

Schematics courtesy of Alexa Baumer, Leftwich laboratory, The George Washington University

A Simplified Physical Experiment

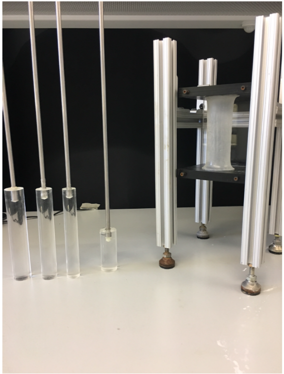

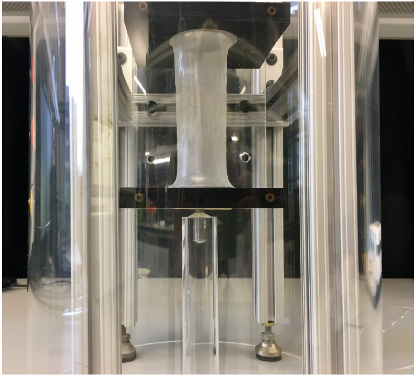

Physical experiment at Leftwich laboratory, The George Washington University

Flow Through Elastic Tubes

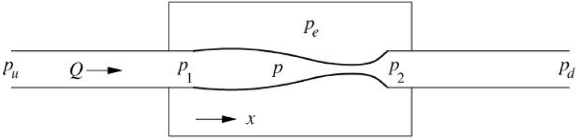

The Starling Resistor [5] model

- elastic tubing mounted at ends on rigid tubes (see figure)
- when approximated by a ring, buckling with *n*-fold symmetry [6,7]
- 3D shell models for elastic tube in Stokes and N-S flow [4]
- fiber tube models mimic muscle architecture with varied buckling behavior [8,9,10]

Figure: [4] Grotberg, Jensen, *Annual Rev. Fluid Mech.*, 2004
[5] Knowlton, Starling, *J. of Physiology*, 1912
[6] Tadjbakhsh, Odeh, *J. of Mathematical Analysis and Applications*, 1967
[7] Flaherty, Keller, Rubinow, *SIAM J. of Applied Math*, 1972
[8] Rosar, Peskin, *New York J. of Math*, 2001
[9] El Hamdaoui, Merodio, Ogden, *International J. of Solids and Structures*, 2015
[10] Qi, Gao, Ogden, Hill, Holzapfel, Han, Luo, *J. of Mech. Behavior of Biomed. Materials*, 2015

Spring Network Model of Elastic Tube

- Tube modeled by network of Hookean springs oriented longitudinally, circumferentially, and helically.
- Force at point $\mathbf{x}_l$ due to spring from point $\mathbf{x}_m$:
  $\mathbf{g}(\mathbf{x}_l) = \tau \left(\frac{\|\mathbf{x}_m - \mathbf{x}_l\|}{\Delta_{lm}} - 1 \right) \frac{(\mathbf{x}_m - \mathbf{x}_l)}{\|\mathbf{x}_m - \mathbf{x}_l\|}$
- Total force due to springs at the points $\mathbf{x}_l$ is the sum of forces from 10 to 16 springs connected to $\mathbf{x}_l$.

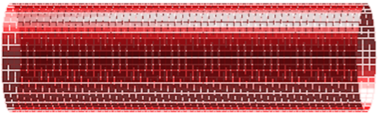

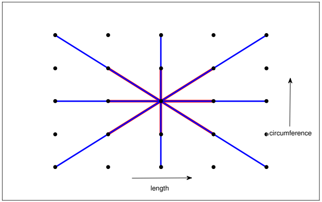

Spring Network Model of Elastic Tube

Total elastic energy stored in the discrete spring system [11]:

$$E_n = \sum_{\text{springs}} \frac{\tau}{2\Delta_{lm}} \left(||\mathbf{x}_m - \mathbf{x}_l|| - \Delta_{lm} \right)^2$$

where τ is the spring constant of every spring, Δ_{lm} is the spring resting length.

Total elastic energy stored in a homogeneous elastic tube [12]:

$$E = \frac{1}{2} A \beta^2 L$$

where $A = \mathcal{E} I$ is the bending stiffness of the tube, $\mathcal{E}$ is the tube's Young's modulus, I is the tube's second moment of area, β its curvature, and L its length.

By enforcing $E_n = E$ for various curvatures β, we can relate individual spring stiffness to macroscopic elastic energy to choose τ.

[11] Nguyen, Fauci. *J. of The Royal Soc. Interface*, 2014
[12] Kelly. 2013

Modeling Fluid Structure Interaction

Low Reynolds number in physical experiment $\rightarrow$ Stokes equations:

$$
\begin{aligned}
0 &= \mu \Delta \mathbf{u} - \nabla p + \mathbf{f}_0 \delta(\mathbf{x} - \mathbf{x}_0) \\
0 &= \nabla \cdot \mathbf{u}
\end{aligned}
$$

Fundamental solution, Stokeslet:

$$
\begin{aligned}
\mathbf{u}(\mathbf{x}) &= \frac{1}{\mu}(\mathbf{f}_0 \cdot \nabla)\nabla B - \mathbf{f}_0 G \\
&= \frac{1}{8\pi\mu}\left(\frac{\mathbf{f}_0}{||\mathbf{x} - \mathbf{x}_0||} + \frac{(\mathbf{f}_0 \cdot \mathbf{x})\mathbf{x}}{||\mathbf{x} - \mathbf{x}_0||^3}\right)
\end{aligned}
$$

where $\Delta G = \delta(\mathbf{x} - \mathbf{x}_0), \Delta B = G$.

Regularization of Stokes Equations

Some numerical difficulty can be resolved by using regularization to eliminate the singularity in $\mathbf{u}$ at $\mathbf{x}_0$ due to force $\mathbf{f}_0$.

Method of regularized Stokeslets [13]
- consider Stokes equations for regularized forces

$$
\begin{aligned}
0 &= \mu \Delta \mathbf{u} - \nabla p + \mathbf{f}_0 \phi_\varepsilon(\mathbf{x} - \mathbf{x}_0) \\
0 &= \nabla \cdot \mathbf{u}
\end{aligned}
$$

where the blob function ϕ_ε satisfies $\int \phi_\varepsilon \, \mathrm{d}\mathbf{x} = 1$ and

$$
\lim_{\varepsilon \to 0} \langle \phi_\varepsilon, \psi \rangle = \langle \delta, \psi \rangle
$$

for any test function ψ (integrable, with compact support).

[13] Cortez, *SIAM J. Sci. Comp.*, 2001

Regularization of Stokes Equations

Stokes equations for regularized forces:

$$
\begin{aligned}
0 &= \mu\Delta\mathbf{u} - \nabla p + \mathbf{f}_0\phi_\varepsilon(\mathbf{x}-\mathbf{x}_0) \\
0 &= \nabla\cdot\mathbf{u}
\end{aligned}
$$

Solution to regularized Stokes equations:

$$\mathbf{u}(\mathbf{x}) = \frac{1}{\mu}(\mathbf{f}_0\cdot\nabla)\nabla B\varepsilon - \mathbf{f}_0 G_\varepsilon$$

where $\Delta G_\varepsilon = \phi_\varepsilon(\mathbf{x}-\mathbf{x}_0), \Delta B_\varepsilon = G_\varepsilon$.

We use the blob function $\phi_\varepsilon = \frac{15\varepsilon^4}{8\pi(||\mathbf{x}-\mathbf{x}_0||^2+\varepsilon^2)^{(7/2)}}$. [14]

[14] Cortez, Fauci, Medovikov, *Physics of Fluids*, 2005

Algorithm

Using the solution to the regularized Stokes equations $\mathbf{u} = A\mathbf{f}$

(1) Calculate spring forces in the tube based on its deformation. Calculate the velocity they induce on the inner cylinder and fixed tube ends (matrix multiplication).

(2) Solve for additional forces necessary on inner cylinder and tube ends to achieve prescribed velocities, using BiCGSTAB iterative method to solve linear system. [15]

(3) Evaluate the velocity at points on tube (matrix multiplication).

(4) Update the tube and rod positions using these velocities and prescribed velocities one step forward in time, using Forward Euler time-stepping.

(5) Repeat.

[15] Van der Vorst, *SIAM J. Sci. Stat. Comput.*, 1992

Model Validation and Regularization Parameter Choice

For concentric rigid cylinders of infinite length, with outer tube of radius R_T fixed and inner cylinder of radius R_C moving at constant velocity U:

- Velocity profile between cylinders is given by: $u(r) = \frac{U(\ln(R_t) - \ln(r))}{\ln(R_t) - \ln(R_c)}$
- Traction at a point on the side of inner cylinder is: $t = \frac{\mu U}{R_c \ln\left(\frac{R_T}{R_C}\right)}$
- Compared to numerical results for finite-length concentric rigid cylinders:

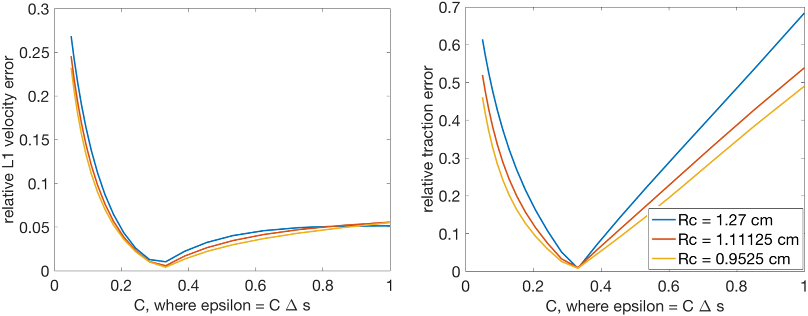

Model Validation and Regularization Parameter Choice

For concentric rigid cylinders of infinite length, with outer tube of radius R_T fixed and inner cylinder of radius R_C moving at constant velocity U:

- Velocity profile between cylinders is given by: $u(r) = \frac{U(\ln(R_t) - \ln(r))}{\ln(R_t) - \ln(R_c)}$
- Traction at a point on the side of inner cylinder is: $\tau = \frac{\mu U}{R_c \ln\left(\frac{R_T}{R_C}\right)}$
- Compared to numerical results for finite-length concentric rigid cylinders:

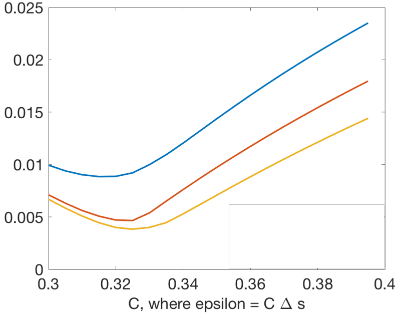

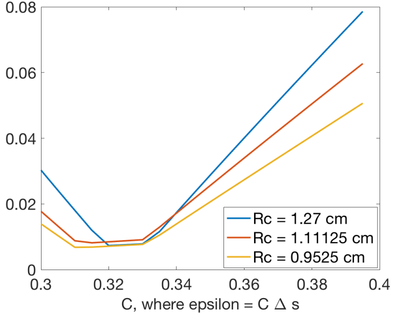

A case study

Inner cylinder through elastic tube, from side

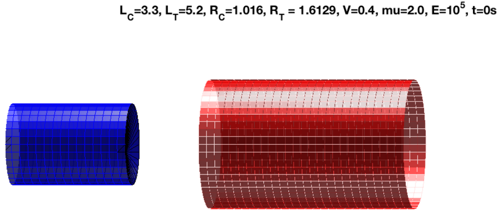

A case study

Inner cylinder through elastic tube, from end

L_C=3.3, L_T=5.2, R_C=1.016, R_T = 1.6129, V=0.4, mu=2.0, E=10^5, t=0s

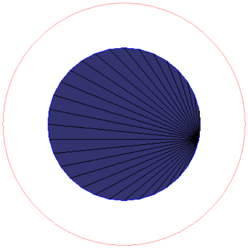

A case study

Fluid pressure

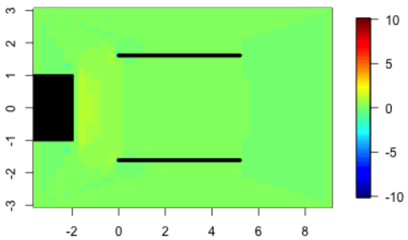

Fluid velocity

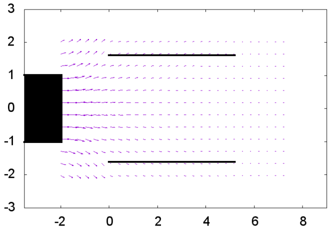

A case study

Longitudinal strain

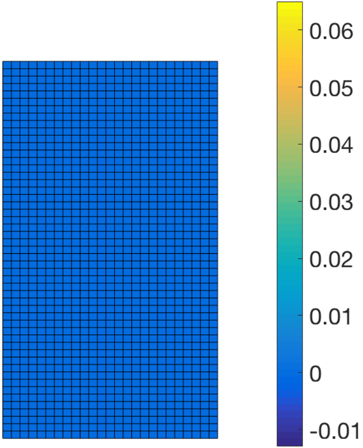

Circumferential strain

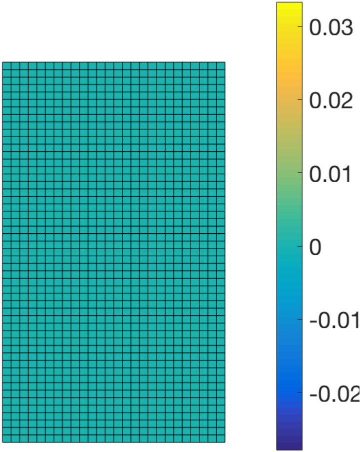

A case study

Longitudinal strain

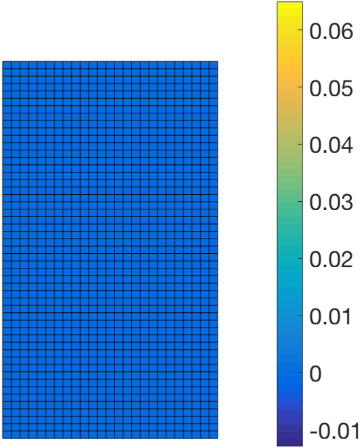

Circumferential strain

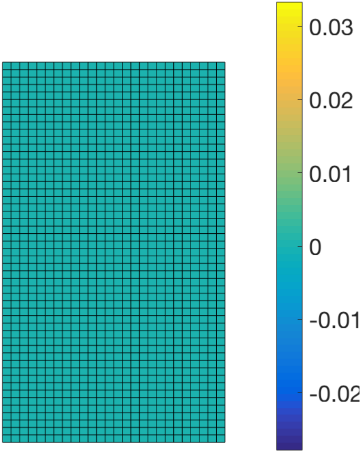

A case study

Tube deformation over time

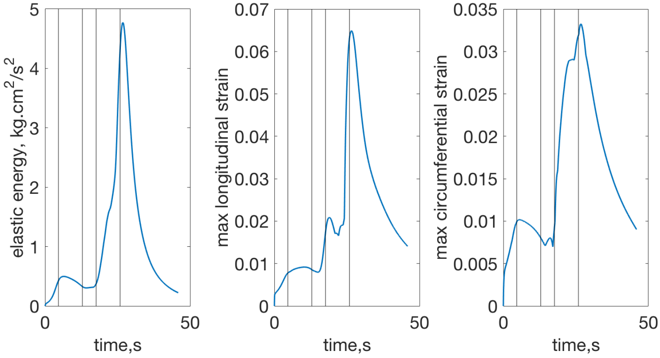

A case study

Force on inner cylinder to achieve prescribed velocity

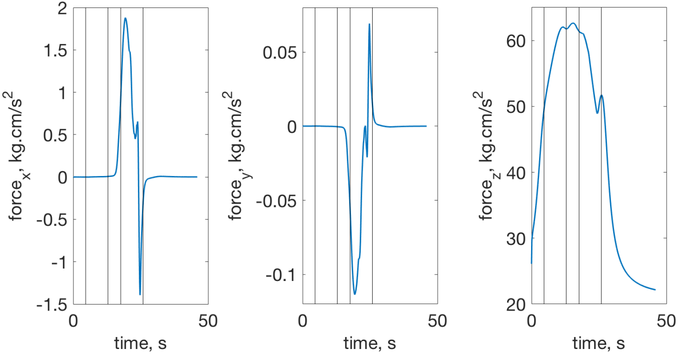

Effect of varying velocity

Force on inner cylinder to achieve varying prescribed velocity

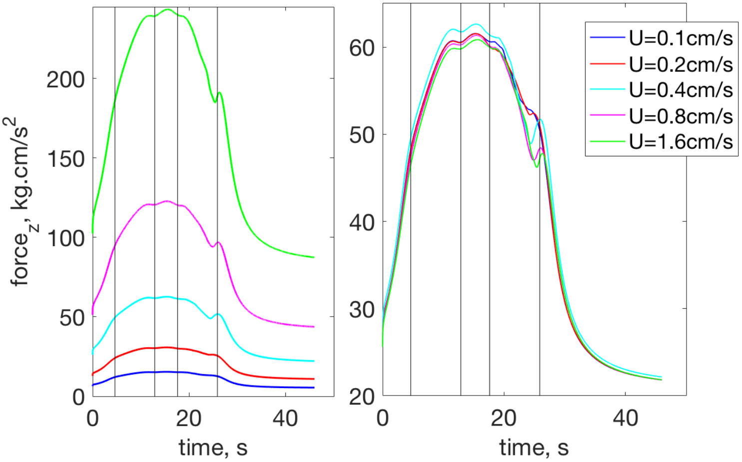

Effect of varying velocity

Tube deformation for varying prescribed velocity

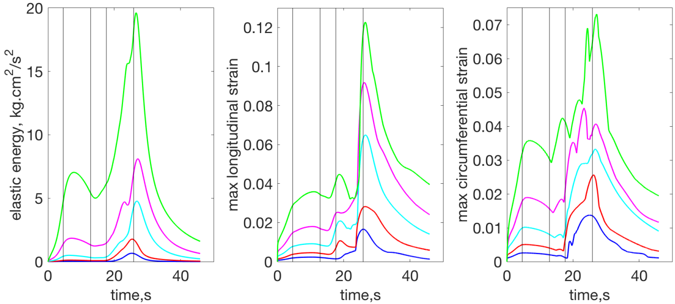

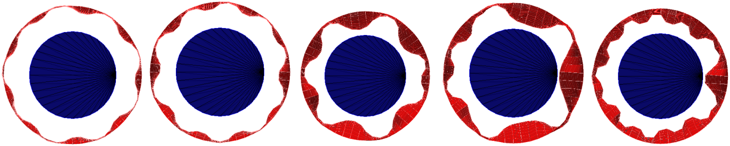

U=0.1 U=0.2 U=0.4 U=0.8 U=1.6

Algorithm 2 (no prescribed velocity)

A modification:

- force input is more realistic for biological applications than prescribed velocity
- force input gives us the freedom to activate the tube

we build an elastic spring cylinder, with every point connected to every other point by a spring with force

$$\mathbf{g}_c(\mathbf{x}_l) = \tau_c \left(\frac{\|\mathbf{x}_m - \mathbf{x}_l\|}{\Delta_{lm}} - 1 \right) \frac{(\mathbf{x}_m - \mathbf{x}_l)}{\|\mathbf{x}_m - \mathbf{x}_l\|}$$

and we anchor the tube ends with forces that penalize moving away from their initial positions

$$\mathbf{g}_p(\mathbf{x}_l) = \tau_p ||\mathbf{x}_m - \mathbf{x}_l||(\mathbf{x}_m - \mathbf{x}_l)$$

Algorithm 2 (no prescribed velocity)

Using the solution to the regularized Stokes equations $\mathbf{u} = A\mathbf{f}$

(1) Calculate spring forces in the tube and in the inner cylinder based on their deformation.

(2) Calculate penalty forces on tube ends based on their position.

(3) Add prescribed forces to inner cylinder to “push” it through the tube.

(3) Evaluate the velocity at points on tube and inner cylinder (matrix multiplication).

(4) Update the tube and rod positions using these velocities and prescribed velocities one step forward in time, using Forward Euler time-stepping.

(5) Repeat.

Algorithm 2 (no prescribed velocity)

Benefits

- speed
  - Method #1: BiCGSTAB + $2[A\mathbf{f}] = O(Nn^2)$ flops,
    where N = number of iterations to convergence of linear solver at each time step (≈ 100),
    n = number of rows in A
  - Method #2: $[A\mathbf{f}] = O(n^2)$ flops, also linear speed-up
  - Small sample problem ($n = 6396$, assume $N = 100$):
    - 8.27×10^9 vs. 4.09×10^7
- any force input

Inner cylinder alignment

Inner cylinder shifted 0.25 cm toward tube wall

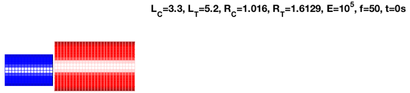

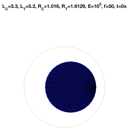

Inner cylinder alignment

Inner cylinder shifted 0.25 cm toward tube wall

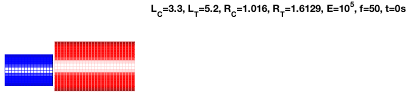

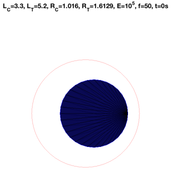

Inner cylinder alignment

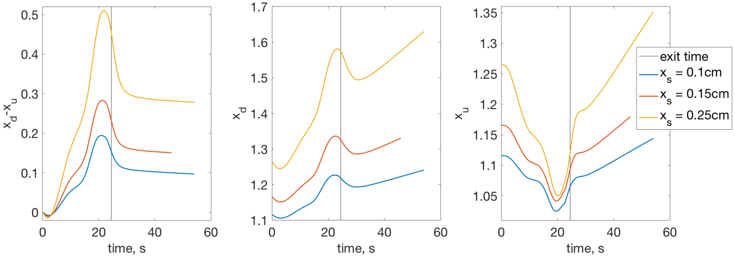

Peristaltic contractions - periodic velocity input

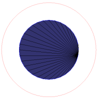

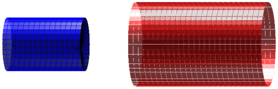

Peristaltic contractions - periodic velocity input

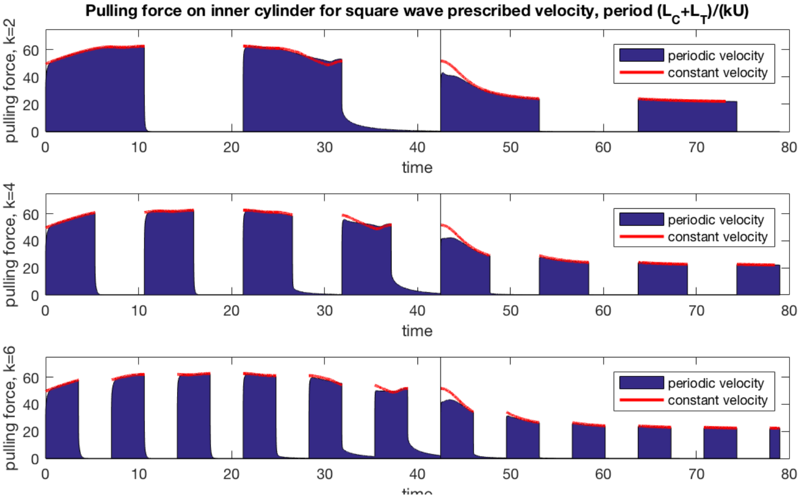

Peristaltic contractions - periodic force input

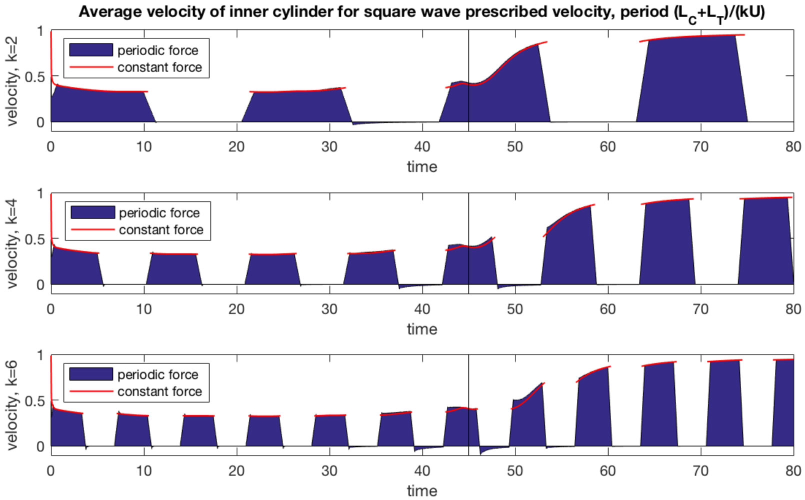

Peristaltic contractions - contracting tube

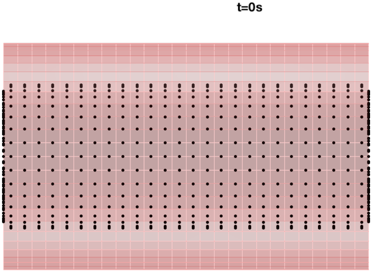

Peristaltic contractions - contracting tube

L_C=3.3, L_T=5.2, R_C=1.016, R_T=1.6129, E=10^5, f=1, U=2, t=0s

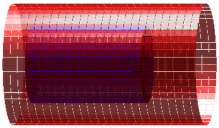

Peristaltic contractions - contracting tube

Effect on average velocity of inner cylinder of varying parameters

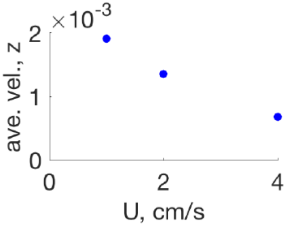

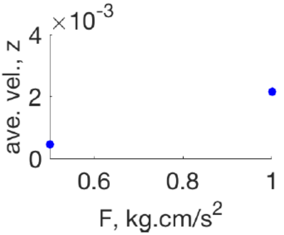

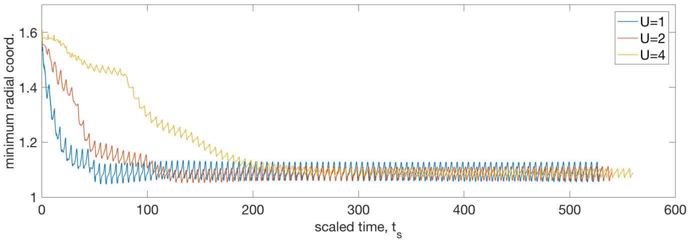

Decreased inner cylinder velocity with increased contraction speed

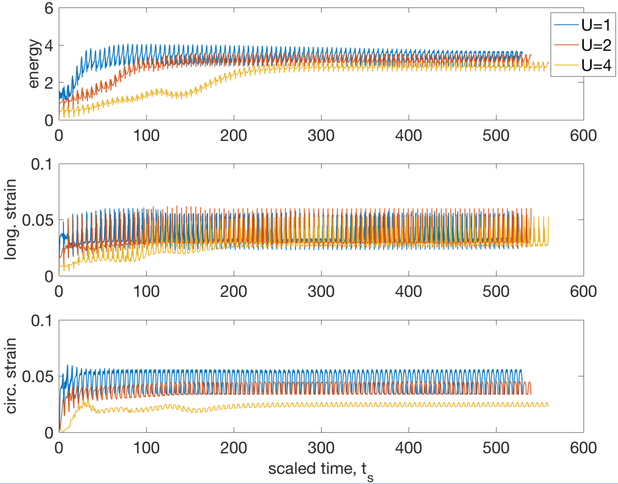

Peristaltic contractions - contracting tube

Tube deformation for varying contraction force

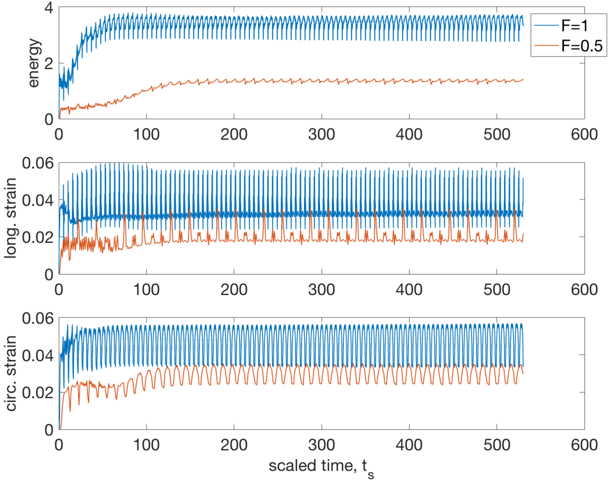

Tube number

We aim to find a "tube number" similar to the "sperm number" used to classify buckling in elastic fibers, in order to predict tube buckling behavior.

Similar in form to

- $\eta_1 = \Lambda \left(\frac{\xi_\perp}{TA} \right)^{1/4}$
  where Λ is the wave length of the buckling, $\xi_\perp$ is a perpendicular resistance coefficient, T is a characteristic time, A is the bending rigidity of the fiber [16]
- $\eta_2 = \frac{8\pi\mu\dot{\gamma}L^4}{-\log(\lambda^2 e)A}$
  where μ is fluid viscosity, $\dot{\gamma}$ is a strain rate, λ is fiber's aspect ratio [17]

[16] Lauga, Eloy, *J. Fluid Mech.*, 2013
[17] Yang, Fauci, *J. Fluid Mech.*, 2017

Tube number

$$\eta = \frac{\xi_\perp \dot{\gamma} L^4}{\mathcal{E} I} = \frac{\mu U L_T^4}{(R_T - R_C) R_T \ln\left(\frac{R_T}{R_C}\right) h^3 \mathcal{E}}$$

where μ is fluid viscosity, U inner cylinder velocity, L_T tube length, R_T tube radius, R_C inner cylinder radius, h tube wall thickness, $\mathcal{E}$ Young's modulus of tube

Tube number

Elastic dynamics creates nonlinear relationship between forces and velocity, despite linearity of Stokes equations.

Non-dimensionalizing the Stokes equations:

$$
\begin{gathered}
0 = -\nabla^* p^* + \mu \Delta^* \mathbf{u}^*, \\
\text{Let } p^* = \mathcal{E} p, \mathbf{x}^* = L\mathbf{x}, \mathbf{u}^* = U\mathbf{u} \\
\implies 0 = -\nabla p + \frac{\mu U}{L\mathcal{E}} \Delta \mathbf{u}
\end{gathered}
$$

where μ is fluid viscosity, U is a characteristic velocity, L a characteristic length, $\mathcal{E}$ the Young's modulus of the tube, p is fluid pressure, $\mathbf{u}$ is fluid velocity [13]

Using dimensional analysis, we can show

$$
f = \frac{\mu^2 U^2}{\mathcal{E}} \zeta \left(\frac{\mu U}{\mathcal{E} R_C}, \frac{\mu U}{\mathcal{E} R_T}, \frac{\mu U}{\mathcal{E} L_C}, \frac{\mu U}{\mathcal{E} L_T} \right)
$$

For a set system geometry and fixed $\mu U/\mathcal{E}$, $f = C\mu U$.

Thus linearity is restored to the system.

Tube number

For constant η, linear force-velocity relationship...

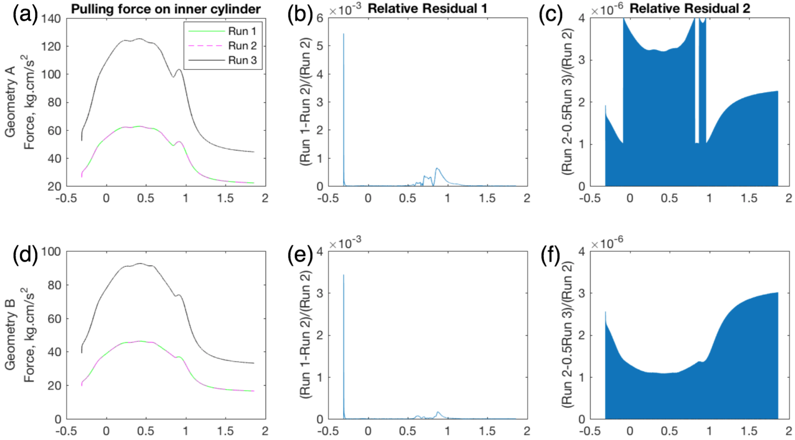

...and invariant elastic buckling.

Tube number

Effect of varying η

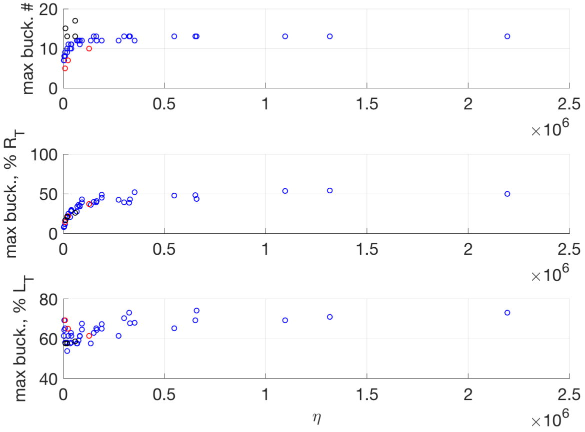

Blue:
$R_T \approx 1.613$
Red:
$R_T \ll 1.613$
Black:
$R_T \gg 1.613$

Conclusions

- Preliminary model of human birth so far used to
  - relate size, velocity, and initial position of inner cylinder to forces on inner cylinder and strain and deformation in tube
  - activate tube with peristaltic contractions
  - predict tube buckling behavior based on system parameters
- Future developments
  - biologically based model of birth canal (closed end, muscle structure)
  - rheological properties of amniotic fluid and other involved fluids
  - shape and elasticity of 'fetus'
- End goal:
  - a numerical model able to predict the circumstances under which vaginal birth can progress successfully, and when it may become unsafe

References

[1] R. A. Brace and E. J. Wolf. Normal amniotic fluid volume changes throughout pregnancy. *American Journal of Obstetrics and Gynecology*, 161(2):382-88, 1989.

[2] D. Uyeno. The physical properties and chemical composition of human amniotic fluid. *Journal of Biological Chemistry*, 37(1):77-103, 1919.

[3] A. M. Lehn, A. Baumer, and M. C. Leftwich. An experimental approach to a simplified model of human birth. *Journal of Biomechanics*, 49(11):2313-17, 2016.

[4] F. P. Knowlton and E. H. Starling. The influence of variations in temperature and blood-pressure on the performance of the isolated mammalian heart. *The Journal of Physiology*, 44(3):206-19, 1912.

[5] J. B. Grotberg and O. E. Jensen. Biofluid mechanics in flexible tubes. *Annual Review of Fluid Mechanics*, 36:121-47, 2004.

[6] I. Tadjbakhsh and F. Odeh. Equilibrium states of elastic rings. *Journal of Mathematical Analysis and Applications*, 18(1):59-74, 1967.

References

[7] J. E. Flaherty, J. B. Keller, and S. I. Rubinow. Post buckling behavior of elastic tubes and rings with opposite sides in contact. *SIAM Journal of Applied Math*, 23(4):446-55, 1972.

[8] M. E. Rosar and C. S. Peskin. Fluid flow in collapsible elastic tubes: a three-dimensional numerical model. *New York Journal of Math*, 7:281-302, 2001.

[9] M. El Hamdaoui, J. Merodio, and R. W. Ogden. Loss of ellipticity in the combined helical, axial and radial elastic deformations of a fibre-reinforced circular cylindrical tube. *International Journal of Solids and Structures*, 63:99-108, 2015.

[10] N. Qi, H. Gao, R. W. Ogden, N. A. Hill, G. A. Holzapfel, H. C. Han, and X. Luo. Investigation of the optimal collagen fibre orientation in human iliac arteries. *Journal of the Mechanical Behavior of Biomedical Materials*, 52:108-19, 2015.

[11] H. Nguyen and L. Fauci. Hydrodynamics of diatom chains and semi flexible fibres. *J. of Royal Soc. Interface*, 11(96):20140314, 2014.

References

[12] P. Kelly. Solid mechanics part i: An introduction to solid mechanics, 2013. `http://homepages.engineering.auckland.ac.nz/~pkel015/SolidMechanicsBooks/Part_I`.

13] R. Cortez. The method of regularized Stokeslets. *SIAM Journal on Scientific Computing*, 23(4):1204-25, 2001.

[14] R. Cortez, L. Fauci, and A. Medovikov. The method of regularized Stokeslets in three dimensions: analysis, validation, and application to helical swimming. *Physics of Fluids*, 17(3):031504, 2005.

[15] H. A. Van der Vorst. Bi-CGSTAB: A fast and smoothly converging variant of Bi-CG for the solution of nonsymmetric linear systems. *SIAM Journal on Scientific and Statistical Computing*, 13 (2), 631-44, 1992.

[16] E. Lauga and C. Eloy. Shape of optimal active flagella. *Journal of Fluid Mechanics*, 730, 2013.

[17] Q. Yang and L. Fauci. Dynamics of a macroscopic elastic fibre in a polymeric cellular flow. *Journal of Fluid Mechanics*, 817:388-405, 2017.

t=0s